High peak and high average radiofrequency power transmit/receive switch for Thermal Magnetic Resonance

Yiyi Ji[1], Werner Hoffmann[2], Michal Pham[1], Alexander E. Dunn[3], Haopeng Han[1], Celal Özerdem[1], Helmar Waiczies[4], Michael Rohloff[1], Beate Endemann[1], Cyrille Boyer[3], May Lim[3], Thoralf Niendorf[1,5] and Lukas Winter[1]

[1] Berlin Ultrahigh Field Facility (B.U.F.F.), Max Delbrück Center for Molecular Medicine in the Helmholtz Association (MDC), Berlin, Germany,

[2] Physikalisch-Technische Bundesanstalt (PTB), Berlin, Germany,

[3] School of Chemical Engineering, The University of New South Wales, Sydney, Australia,

[4] MRI.TOOLS GmbH, Berlin, Germany,

[5] Experimental and Clinical Research Center (ECRC), a joint cooperation between the Charité Medical Faculty and the Max Delbrück Center for Molecular Medicine in the Helmholtz association, Berlin, Germany.

Corresponding author:

Dr. Lukas Winter
Berlin Ultrahigh Field Facility (B.U.F.F.)
Max-Delbrück Center for Molecular Medicine
Robert-Rössle-Strasse 10
13125 Berlin
Germany
Tel.: +49 30 9406 4546
E-mail:Lukas.Winter@mdc-berlin.de

Citation:

Ji Y, Hoffmann W, Pham M, et al. High peak and high average radiofrequency power transmit/receive switch for thermal magnetic resonance. *Magn Reson Med*. 2018;00:1–10. https://doi.org/10.1002/mrm.27194

ABSTRACT

Purpose: To study the role of temperature in biological systems, diagnostic contrasts and thermal therapies, radiofrequency (RF) pulses for magnetic resonance (MR) spin excitation can be deliberately used to apply a thermal stimulus. This application requires dedicated transmit/receive (Tx/Rx) switches that support high peak powers for MRI and high average powers for RF heating. To meet this goal, we propose a high-performance Tx/Rx switch based on PIN diodes and quarter-wavelength (λ/4) stubs.

Methods: The λ/4 stubs in the proposed Tx/Rx switch design route the transmitted RF signal directly to the RF coil/antenna without passing through any electronic components (e.g. PIN diodes). Bench measurements, MRI, MR thermometry and RF heating experiments were performed at f=297MHz (B_0=7.0T) to examine the characteristics and applicability of the switch.

Results: The proposed design provided an isolation of -40.0dB/-41.5dB during transmission/reception. The insertion loss was -0.41dB/-0.27dB during transmission/reception. The switch supports high peak (3.9kW) and high average (120W) RF powers for MRI and RF heating at f=297MHz. High-resolution MRI of the wrist yielded image quality competitive with that obtained with a conventional Tx/Rx switch. RF heating in phantom monitored by MR thermometry demonstrated the switch applicability for thermal modulation. Upon these findings, thermally activated release of a model drug attached to thermoresponsive polymers was demonstrated.

Conclusion: The high-power Tx/Rx switch enables thermal MR applications at 7.0T, contributing to the study of the role of temperature in biological systems and diseases. All design files of the switch will be made available open source on www.opensourceimaging.org.

Key words: thermal magnetic resonance, transmit receive switch, ultrahigh field MR, RF induced heating, open source hardware

1. INTRODUCTION

Temperature is a physical parameter with diverse biological implications and intense clinical interest. Controlled increase of temperature has been used in thermal therapies. Mild hyperthermia performed at temperatures of T=41-45°C is a potent sensitizer for chemo- and radiotherapies (1-5). Smart drug carriers that release their load after a temperature stimulus are employed to deliver chemotherapeutics specifically to the target site, increasing the therapeutic dose and minimizing systemic toxicity (6,7). Other (bio)molecules have been loaded to thermoresponsive carriers for delivery and controlled release, such as magnetic resonance imaging (MRI) contrast agents (8,9), genes (10,11) and peptides/proteins (12).

MRI is a valuable tool for diagnosis, treatment planning and treatment control of thermal interventions including the spectrum of diagnostic imaging and non-invasive temperature monitoring (13-16). It has been demonstrated that radiofrequency (RF) pulses tailored for spin excitation can also be employed for the application of a thermal stimulus (17). This approach denoted as thermal MR (18-20) uses the pulsed power amplifier of the MR system together with dedicated RF antenna arrays to generate RF induced focal thermal modulation.

Performing MRI and RF heating simultaneously requires high peak power (>1kW) and high average power (>100W per channel), support of the RF antennae as well as other RF hardware components. While RF antennae have already been developed for thermal MR (17-20), high peak and high average RF power transmit/receive (Tx/Rx) switches that switch between high power (kW) transmission to low power (μW) reception of the MR signal are still lacking.

MR Tx/Rx switches deploy positive-intrinsic-negative (PIN) diodes as active switching units, as they offer very low resistance in forward biased state, high isolation in the reverse bias state, fast switching time and high peak power handling (21). PIN diodes have been incorporated in various designs for different purposes: high isolation (22), ultra-short switching time (23), double-tuned nuclei in linear/quadrature mode (24) and miniaturized Tx/Rx switches (25). Although all these designs are capable of handling high peak power for MRI, their average power handling (e.g. at high duty cycles) is limited typically by electronic components (e.g. PIN diodes) placed in the

transmission path. Thus the overall applicable average power is limited severely in order to avoid excessive heat accumulation in these components.

In this work, we propose a high peak and high average power Tx/Rx switch design that supports MRI and high-power RF heating in thermal MR applications at 297MHz (B_0=7.0T). The proposed switch was benchmarked against a conventional Tx/Rx switch. Diagnostic *in vivo* MRI, RF heating and temperature induced release of a model drug from a thermoresponsive polymer in a phantom demonstrate the potential range of applications of the proposed Tx/Rx switch.

2. METHODS

2.1 Hardware design

The electrical circuit of the proposed high-power Tx/Rx switch for 7.0T (*f*=297MHz) (26) is shown in **Fig.1a** with a photograph of the assembled switch shown in **Fig.1b**. In the proposed single pole double through (SPDT) design, no electronic components are placed in the direct transmission path (27) (**Fig.1c**). Consequently, excessive heat accumulation during high duty cycle high-power RF pulse transmission is avoided and higher peak and average powers can be applied.

During transmission, the PIN diodes D1 and D2 (MA4P7441F-1091T, Macom, MA, USA) are forward biased (U_{DC}=5V, I=100mA). The low impedance at points 1 and 4 (**Fig.1c)** is transformed by the λ/4 stubs into high impedance at points 2 and 3, routing the RF pulse from the Tx port directly to the RF coil/antenna without passing through the PIN diodes.

During reception, the PIN diodes are reverse biased (U_{DC}=-30V). The high impedance at point 1 is transformed into low impedance at point 2 and again to high impedance at point 3 by the λ/4 stubs, routing the received RF signal from the RF coil/antenna into the Rx port (**Fig.1d**). The Rx port is connected to a low noise preamplifier (LNA) (Siemens Healthineers, Erlangen, Germany).

Capacitors C1=C2=2.4nF and inductors L1=L2=910nH (3650 series, TE connectivity Lda., Schaffhausen, Switzerland) were used to block direct current (DC) and RF, respectively. C1 and C2, consisted each of five parallel 470pF ceramic capacitors (700E, American Technical Ceramics, Huntington Station, NY, USA), were soldered under a copper plate (25x40x2)mm^3. The PIN diodes D1 and D2 were soldered on top of these copper plates for heat dissipation (**Fig.1b**). The parallel circuit L3+C3 tuned to 297MHz creates DC ground for D1 and blocks RF from DC ground. The inductor L4=910nH (3650 series, TE connectivity Lda., Schaffhausen, Switzerland) creates DC ground for D2 and acts as an RF choke (measured reactance of 1.76kΩ @ 300MHz) (28). The cable shield of the λ/4 stubs is connected to ground at point A (**Fig.1a**). At point B, a frequency selective RF ground is provided by the series resonant circuit L5+C4,

with L5 being the self-inductance of the cable shield. For L3=46nH, three windings (inner diameter=4.5mm) of 1mm silver coated copper wire were used. C3=1-8pF and C4=1-40pF are non-magnetic trimmer capacitors (Voltronics Corporation, Salisbury, MA, USA). The λ/4 stubs (L=15.5cm) were assembled with semi-rigid coaxial cable (Sucoform 141 Cu 50Ω, Huber+Suhner AG, Herisau, Swizerland) for 297MHz. In comparison to flexible cables, semi-rigid cables have better dielectric properties, better shielding quality and a more stable phase relation. The two RF branches and associated PIN diodes were placed in double shielded compartments to increase isolation (**Fig.1a-b**). These compartments 1 and 2 can furthermore be characterized, calibrated or modified individually in a modular way. This is possible due to the placement of L4 (which otherwise might not be needed, since DC ground for D2 might also be provided through L3).

The whole circuit was placed on a (110x135x2)mm^3 double sided copper board, which also served as shielding and mounted in a (165x125x75)mm^3 casing.

The isolation and insertion loss of the Tx/Rx switch were assessed by measuring the scattering parameters using a vector network analyzer (ZVT8, Rhode&Schwarz GmbH&Co.KG, Memmingen, Germany).

The switching time between transmission and reception modes was measured using a digital oscilloscope (HMO3524, Hameg Instruments GmbH, Mainhausen, Germany) and a signal generator (SMGL, Schwarz GmbH&Co.KG, Memmingen, Germany).

2.2 High RF power handling test

To evaluate the Tx/Rx switch under high average power conditions, P_{avg}=100W and P_{peak}=1kW (4ms rect-pulse, TR=40ms, duty cycle=10%, generated by an MR RF power amplifier – Stolberg HF Technik AG, Stolberg-Vicht, Germany) was applied to the Tx/Rx switch for 30min and its temperature was monitored with an infrared camera (Ti25, Fluke, WA, USA). For comparison, a conventional 7.0T Tx/Rx switch (Siemens Healthineers, Erlangen, Germany) was used. This switch design has PIN diodes in the transmission path (**Fig.2**) that limit the specified maximum power to P_{avg}=25W.

2.3 Magnetic Resonance Imaging

To demonstrate the suitability of the high-power Tx/Rx switch for MRI, we performed MRI on a human wrist in a B_0=7.0T whole-body MR system (Magnetom, Siemens Healthineers, Erlangen, Germany) using a bow-tie dipole antenna (17,29) for transmission and reception of the RF signal. As a reference, the conventional Tx/Rx switch was applied in the same setup together with the same preamplifier (Siemens Healthineers, Erlangen, Germany). The signal-to-noise ratio (SNR) was calculated by dividing the average signal intensity of a circular ROI drawn in the carpal bones by the standard deviation of the noise from background air. For the *in vivo* feasibility study, subjects were included after due approval by the local ethical committee (registration number DE/CA73/5550/09, Landesamt für Arbeitsschutz, Gesundheitsschutz und technische Sicherheit, Berlin, Germany). Informed written consent was obtained from each volunteer prior to the study in compliance with the local institutional review board guidelines.

2.4 Radiofrequency-induced heating

An experimental setup comprising a rectangular agarose phantom (90x180x260)mm^3 and a bow-tie dipole antenna (**Fig.3a**) was used to examine the suitability of the high-power Tx/Rx switch for RF heating and MR thermometry at 297MHz (B_0=7.0T). The agarose phantom (σ=1.03S/m, ε=71.9) was equipped with seven cylindrical sample holders. Five were located in the RF heated volume governed by a dipole antenna. The remaining two were placed outside of the RF heated volume with ΔT=0°C (**Fig.3b**). The sample holders were filled with 0.1M NaCl solution (σ=1.05S/m, ε=80.4) to avoid susceptibility artifacts. PTFE tubes with inner diameter=1mm were inserted along the long axis of the phantom at depth of 5mm, 15mm, 25mm and 35mm (**Fig.3b-c**) to accommodate fiber optic probes that serve as temperature reference for MR thermometry (MRTh).

RF heating was accomplished using the 7.0T MR system amplifiers at high duty cycle (Magnetom, Siemens Healthineers, Erlangen, Germany). The hardware losses between the transmitter and the feeding point of the dipole antenna was -2.18dB. This setup afforded

P_{peak}=1kW and P_{avg}=100W (4ms rect-pulse, TR=40ms, duty cycle=10%) at the feeding point of the dipole antenna and P_{peak}=1.2kW and P_{avg}=120W at the high-power Tx/Rx switch. The heating paradigm consisted of 3x5min RF heating interleaved with 2D-MRTh acquisition. 2D-MRTh was conducted using a proton resonance frequency shift method (13) in conjunction with a dual gradient-echo technique (14,15). A fiber optic probe (Omniflex, Neoptix, Quebec, Canada) placed 15mm below the bow-tie dipole antenna was used as temperature reference.

For comparison, a conventional Tx/Rx switch was employed using the same heating paradigm with the exception that the average power was limited to P_{avg}=25W at the dipole antenna's feeding point.

2.5 Temperature-induced release of a model drug

To demonstrate a potential application of thermal MR, the experimental setup for RF heating was used for thermally controlled release of molecules from temperature-responsive carriers. For this purpose, a thermoresponsive polymer – P(DEGMA-co-OEGMA-b-[TMSPMA-co-VBA]) (30) was loaded with fluoresceinamine, a fluorescent dye that served as a model for a drug. In this study, the lower critical solution temperature (LCST) (7) of the thermoresponsive polymer is 34°C; at T>34°C, the polymers will contract and become insoluble. This contraction releases the molecules trapped within the polymer layer into the bulk solution.

Solution containing fluoresceinamine loaded polymer was transferred into sample holders of the phantom (**Fig.3b**); i) 9mL of the solution (hereafter referred to as the heated sample) was placed in the center of the hotspot created by the bow-tie dipole antenna, and ii) 9 mL of the solution was placed in a holder outside of the hotspot (the control sample). The distance from the dipole antenna to the phantom increased due to insertion of a tube (diameter=3mm) that would be used to extract the polymer sample. The base temperature in the phantom was maintained at 30°C by a circulating water bath (Thermo Scientific, Waltham, MA, USA).

RF heating of the polymer-fluoresceinamine solution was performed with P_{peak}=1kW and P_{avg}=100W (4ms rect-pulse, TR=40ms, duty cycle=10%) at the antenna feeding point. After 30min, the temperature in the heated sample achieved 40°C while the temperature in the control

sample remained at 30°C. The heated sample was maintained at 40°C for an additional 120min. During this time, small quantities of both heated and control samples were extracted and passed through size exclusion (6kDa) chromatography columns (Bio-Spin 6, Bio-Rad Laboratories, Inc., CA, USA). In our case, the released fluoresceinamine (347Da) would be retained in the gel matrix, while fluoresceinamine still bonded to polymers (15kDa) would be found in the eluate. The eluates were collected and analyzed in a fluorescence reader (GeminiXPS, Molecular Devices, CA, USA).

3. RESULTS

3.1 Transmit/receive switch performance

The proposed high-power Tx/Rx switch provided an isolation of -40.0dB (**Fig.4a**) during transmission and -41.5dB (**Fig.4b**) during reception. The insertion loss was -0.4135dB (**Fig.4c**) during transmission (Tx port – RF coil/antenna) and -0.2732dB (**Fig.4d**) during reception (RF coil/antenna – Rx port). The switching time was approximately 50µs.

After operating at an average power P_{avg}=100W for 30min, the maximum temperature measured in the circuit of the high-power Tx/Rx switch was 58.4°C in the PIN diode D2(**Fig.5a,c**). Applying the same average power, the conventional Tx/Rx switch could only be monitored for a period of 2min, as the temperature in the circuit was already reaching critical levels (97.5°C close to the PIN diode D2' placed in the transmission path) (**Fig.5b,d**).

3.2 Magnetic Resonance Imaging

The high spatial resolution MR images acquired with the high-power Tx/Rx switch (**Fig.6a**) and a conventional Tx/Rx switch (**Fig.6b**) yielded similar image quality. On both images, small structures such as the carpal bones, ulnar disc, radio-carpal joints, ulnar-carpal joints and cartilage could be identified. The SNR was 30.3 for the high-power Tx/Rx switch and 25.4 for the conventional switch. In addition to the MRI experiments, the high-power Tx/Rx switch was tested successfully with the maximum available peak power of the MR system (P_{peak_max}=3930W at the switch).

3.3 Radiofrequency-induced heating

With the applied heating paradigm, the temperature increase in the phantom, as observed by MRTh (**Fig.7a**), was ΔT=5.9°C after 5min, 13.6°C after 10min and 18.5°C after 15min. The

fiber optic probe positioned at the same location registered ΔT=6.7°C after 5min, 12.4°C after 10min and 17.5°C after 15min (**Fig.7b**).

In comparison, the maximum temperature increase in the same location while using a conventional Tx/Rx switch at its limit of P_{avg}=25W was only ΔT=2.3°C after 5min, 4.3°C after 10min and 5.3°C after 15min, as determined by the MRTh temperature map, and ΔT=1.7°C after 5min, 3.5°C after 10min and 4.7°C after 15min registered by the fiber optic probe.

3.4 Temperature-induced release of a model drug

The amount of fluorescenamine released from the thermoresponsive polymers in a heated sample versus a control sample is shown in **Fig.8.** The non-heated control sample released only a small amount of fluorescenamine over a timeframe of 120min. This is due to the slow hydrolysis of Schiff base bonds that attach fluoresceinamine to the polymer at low temperature. The heated sample subject to a temperature above lower critical solution temperature of the polymer (LCST=34°C) showed higher release rate, e.g. 68% after 60min. In this case, the Schiff base bond was hydrolyzed faster at higher temperatures and contraction of the polymer at T>LCST increased the release of fluoresceinamine.

4. DISCUSSION AND CONCLUSION

This work adds to the literature by proposing a high-power Tx/Rx switch which is able to support thermal MR applications of high peak power MRI and high average power RF heating. In our experimental implementation, the high-power switch was able to withstand an average power of P_{avg}=120W and a maximum peak power of P_{peak}=3.9kW. The proposed configuration afforded a low insertion loss of -0.41dB/-0.27dB (transmission/reception) and sufficient isolation of -40dB/-41.5dB (transmission/reception), similar to a commercially available Tx/Rx switch with a measured insertion loss of -0.55dB/-0.32dB (transmission/reception) and isolation of -35.6dB/-46.8dB (transmission/reception). With 50µs, the measured switching time for the high-power switch was slightly lower than for the conventional switch (around 100µs).

The proposed design is simple and fairly low cost. It consists of non-magnetic components allowing it to be placed inside the scanner bore in close proximity to the RF antenna. The strategic placement of the λ/4 stubs routes the RF signal from the transmitter directly to the RF coil/antenna without directly passing through any lossy electronic components such as PIN diodes (27). This enables the use of high average powers in comparison to other Tx/Rx switches designed for MRI applications (22-24). For instance, the conventional Tx/Rx design that was compared in this study uses PIN diodes in the transmission path that have a series resistance of 0.35Ω and 2.2pF. The thermal resistance of these PIN diodes is 5.5 °C/W and the junction temperature is 150 °C. For an ambient temperature of 20 °C, these PIN diodes could only withstand ≈ 24 W. Stud-mounting, heat-sinks and lower resistance PIN diodes might improve the maximum average power handling of this circuit, however it will not be sufficient to increase the applicable power by a factor of more than 4 to above 100W, which is the applicable power of our proposed switch design in this study. The implementation of air or water cooling circuits that provide sufficient cooling is cumbersome in a long bore 7.0T MR scanner.

In L-band radar applications, GaN-HEMT Tx/Rx switches have been presented that facilitate high-power (200W) handling (31). However, the high breakdown voltage requirements for high peak power MR pulses will necessitate the use of multiple transistors per switch, which increases the insertion loss and in particular the costs per switch significantly. These high costs are not

beneficial for the setup of multi-channel (e.g. 16 or 32-channel) transmission system that is needed for thermal MR.

The length of λ/4 stubs is 15.5cm at 7Tesla (f=297MHz). At higher fields, which are in particular interesting for thermal MR applications (19), the size of the λ/4 stubs would be reduced allowing for a more compact switch design. For instance, at B_0=10.5T, f=447MHz, the λ/4 stub size is reduced by approximately 33%.

Using microstrips instead of semi-rigid cables could be another approach to reduce the current size of the high-power Tx/Rx switch, which however could increase transmission losses of the circuit (27,32).

In reception mode ground is well defined by the LNA, however in transmission mode this might not be the case due to the long looped quarter wave coaxial cables used. Thus, the frequency selective ground at location B (**Fig.1a**) is crucial to improve isolation. At the same time interferences with other RF frequencies are reduced. This is of importance for RF heating at higher RF frequencies (e.g. 600MHz) in a hybrid system where MRI and/or RF heating are performed simultaneously at 7.0T (19,33). The frequency selective ground might potentially be affected by the coax cable connecting the antenna to the antenna port of the switch through coupling effects, which might degrade its isolation performance. In order to reduce the influence of the connected coax cable on the switch, either a cable trap at the antenna feeding cable or a trap circuit incorporated into the Tx/Rx switch design at the RF coil/antenna port can be implemented.

High-resolution MRI of the wrist was supported by the high-power switch, with comparable image quality benchmarked against a commercially available Tx/Rx switch. RF heating ($\Delta T>16°C$) and MR thermometry were performed utilizing the high-power switch. The MR thermometry results are well correlated to the readings obtained from fiber optic probes, demonstrating the feasibility of this application without the use of additional cooling circuits for the Tx/Rx switch. These findings allowed the use of the switch for thermally controlled release of a model drug from thermoresponsive polymers in a phantom.

In conclusion, the proposed high-power Tx/Rx switch enables thermal MR applications at 7T, contributing to the study of the role of temperature in biological systems and diseases with

possible implications for diagnosis, treatment and MR safety. In order to facilitate reproducibility and swift dissemination, all design files of the switch will be made available open source on www.opensourceimaging.org.

Acknowledgement

This work was funded in part (Y.J., H.W., L.W.) by the German Federal Ministry of Education and Research (KMU-innovativ: Medizintechnik, FKZ 13GW0102A, FKZ 13GW0102B) and in part (T.N.) by an advanced grant of the European Research Council (ERC AdG 743077).

Conflict of Interest

Thoralf Niendorf is the founder and CEO of MRI.TOOLS GmbH. Helmar Waiczies is an employee of MRI.TOOLS GmbH.

Figures

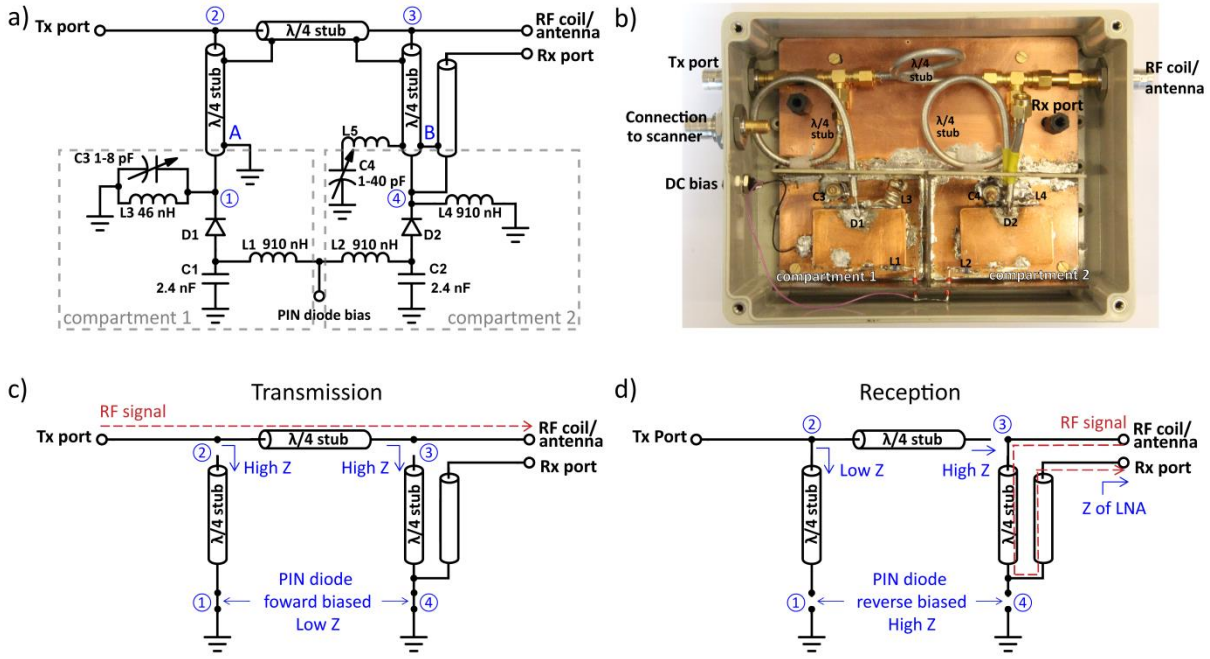

Figure 1 – **a)** Electrical circuit of the proposed high-power Tx/Rx switch. Capacitors C1 and C2 and inductors L1 and L2 were used to block DC and RF, respectively. D1 and D2 are PIN diodes. The parallel circuit L3+C3 (297MHz) creates DC ground for D1 and blocks RF from DC ground. The inductor L4 creates DC ground for D2 and acts as an RF choke. The cable shield of the λ/4 stubs is connected to ground at point A. At point B, a frequency selective RF ground is provided by the series resonant circuit L5+C4, with L5 being the self-inductance of the cable shield. **b)** Photograph of the constructed Tx/Rx switch. The low noise preamplifier board was removed in order to display the full circuit. C1 and C2 (not visible), consisted each of five parallel 470pF ceramic capacitors were soldered under a copper plate (25x40x2)mm^3. The PIN diodes D1 and D2 were soldered on top of these copper plates for heat dissipation. **c)** Equivalent circuit during the transmission mode. The PIN diodes are forward biased; the low impedance at points 1 and 4 is transformed into high impedance at points 2 and 3 by the λ/4 stubs. In this way, the RF signal from Tx port is routed into the RF coil/antenna without passing through PIN diodes. **d)** Equivalent circuit during the receive mode. The PIN diodes are reverse biased; the

high impedance at point 1 is transformed into low impedance at point 2 and again to high impedance at point 3 by the λ/4 stubs, routing the received RF signal from the RF coil/antenna into the Rx port.

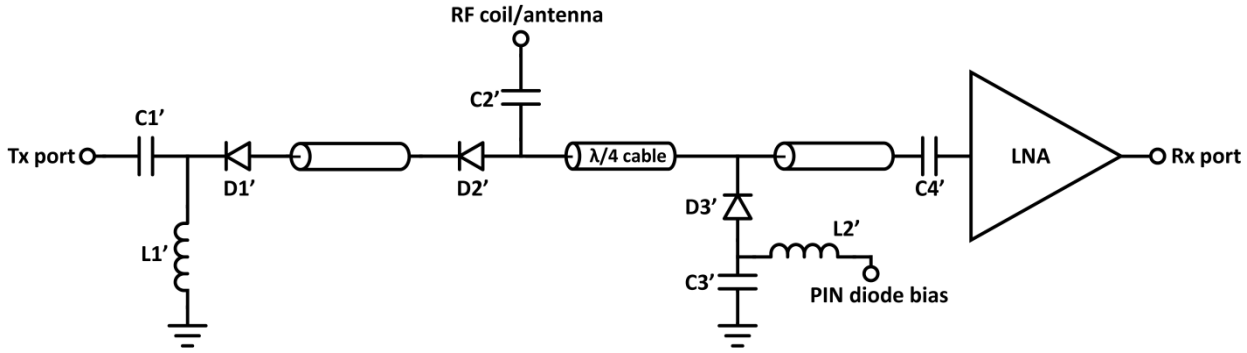

Figure 2 – Simplified circuit schematics of the conventional Tx/Rx switch (Siemens Healthineers, Erlangen, Germany) used in this study. In the transmission mode, all PIN diodes (DH80106, Temex, Pessac, France) are forward biased. D1' and D2' provide a low insertion loss path between Tx port and RF coil/antenna, while the low noise amplifier (LNA) in the receive path is isolated by high impedance transformed by a quarter-wavelength (λ/4) cable from low impedance at D3'. In the receive mode, the PIN diodes are reverse biased, RF signal coming from the RF coil/antenna will be blocked from the Tx port by D1' and D2', and will be directed to the LNA. The measured insertion loss for this switch was -0.55dB/-0.32dB (transmission/reception) and the measured isolation was -35.6dB/-46.8dB (transmission/reception). In this Tx/Rx switch design, all the transmitted RF power passes through the PIN diodes D1' and D2' which is the limiting factor in determining the maximum applicable average power (<25W).

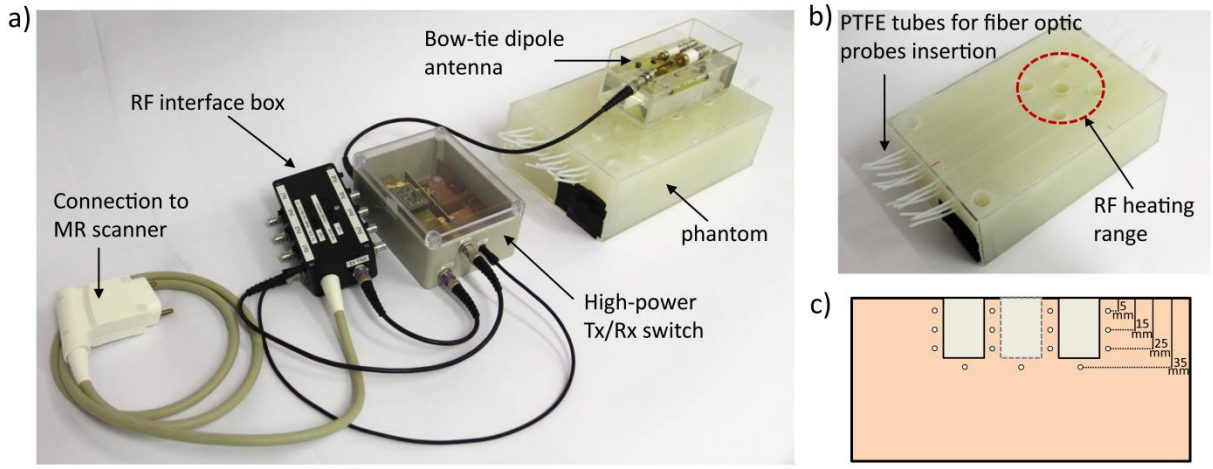

Figure 3 – **a)** Photograph of the RF heating setup consisting of a rectangular agarose phantom ((90x180x260)mm^3, σ=1.03S/m, ε=71.9), a bow-tie dipole antenna, the high-power Tx/Rx switch and an RF interface box. **b)** Photograph of the agarose phantom with seven cylindrical sample holders and fifteen PTFE tubes with inner diameter=1mm for fiber optic temperature probe insertion. The RF heated area is roughly marked by the red dotted circle. **c)** Schematic of the cross section of the phantom with three sample holders and the position of the PTFE tubes at depth of 5mm, 15mm, 25mm and 35mm.

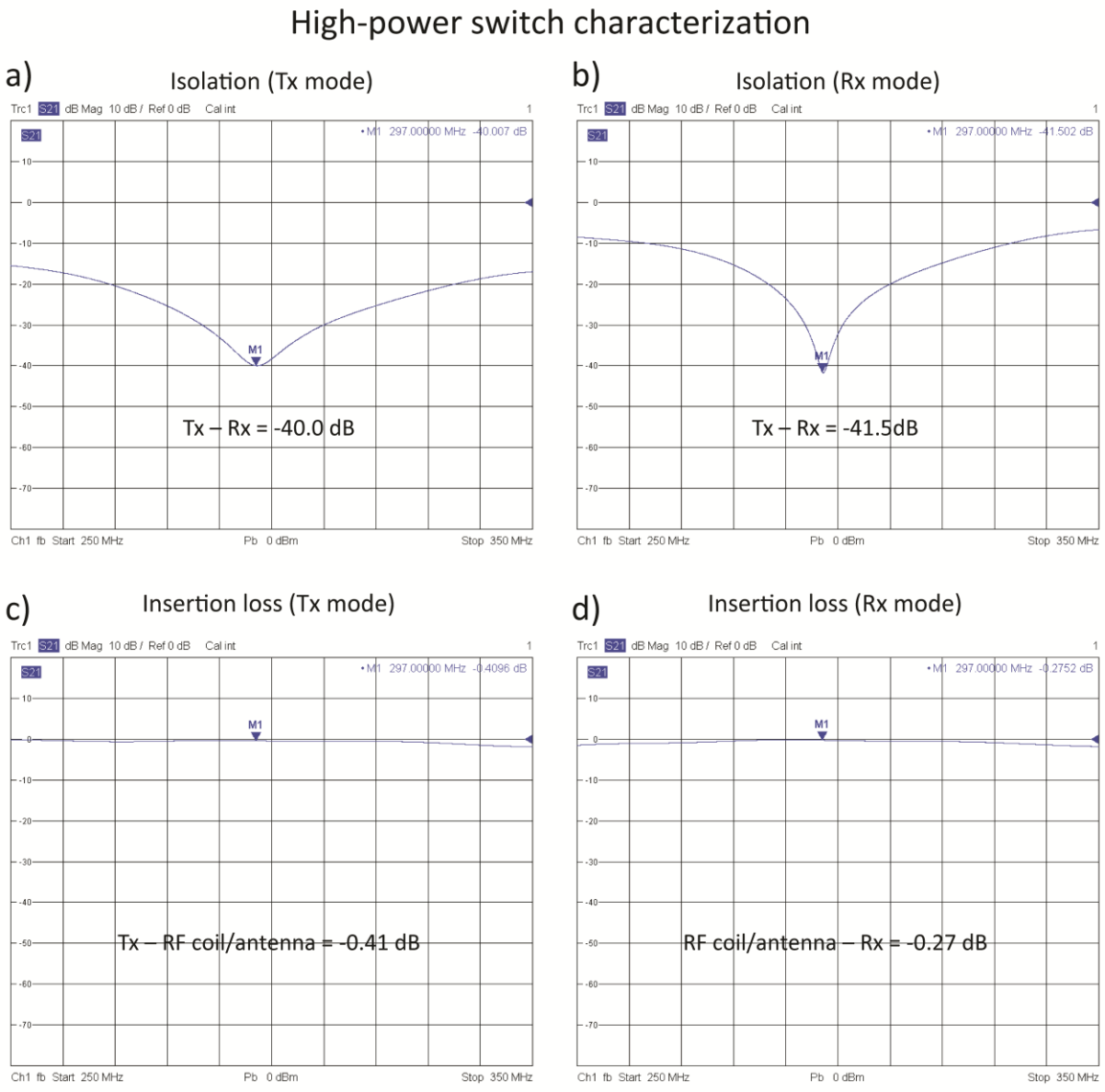

Figure 4 – Network analyzer measurement results of the proposed high-power Tx/Rx switch showing **a)** isolation between Tx port and Rx port (-40.0dB) during transmission, **b)** isolation between the Tx port and Rx port (-41.5dB) during reception **c)** insertion loss between the Tx port and the RF coil/antenna (-0.41dB) during transmission, **d)** insertion loss between the RF coil/antenna and the Rx port (-0.27dB) during reception.

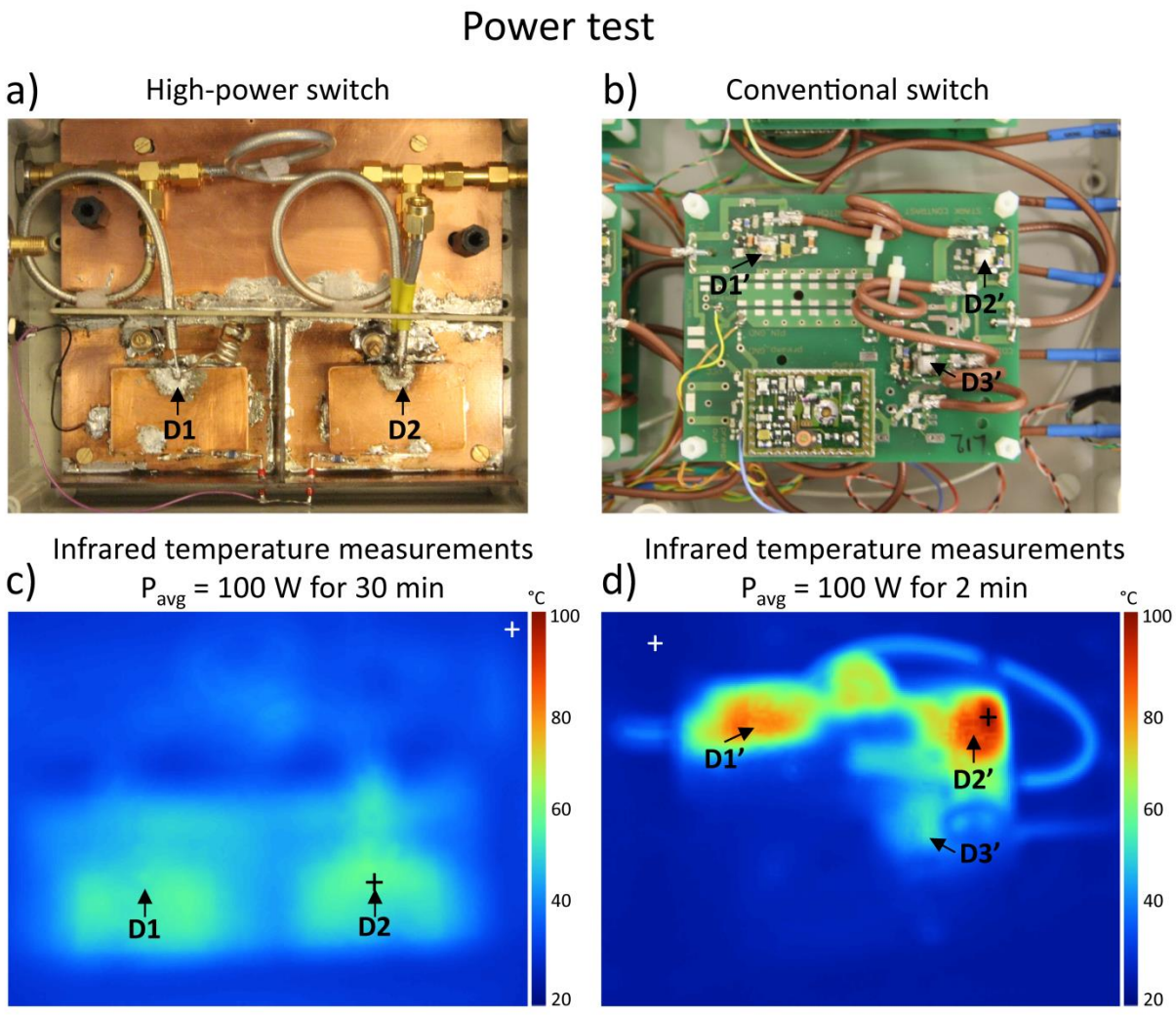

Figure 5 – **a)** Photograph of the high-power Tx/Rx switch circuit. **b)** Photograph of the conventional Tx/Rx switch circuit. Black arrows point to PIN diodes; D1' and D2' are in the transmission path, D3' is in the reception path. **c)** Temperature map acquired with an infrared camera in the high-power Tx/Rx switch after 30min operating at P_{avg}=100W. Background temperature (white +)=28.1°C and highest temperature (black +)=58.4°C (inductor L4). **d)** Temperature map acquired with an infrared camera in the conventional Tx/Rx switch after only 2min operating at P_{avg}=100W. Background temperature (white +)=24.9°C. The highest temperature (black +)=97.5°C was found around the PIN diode D2'.

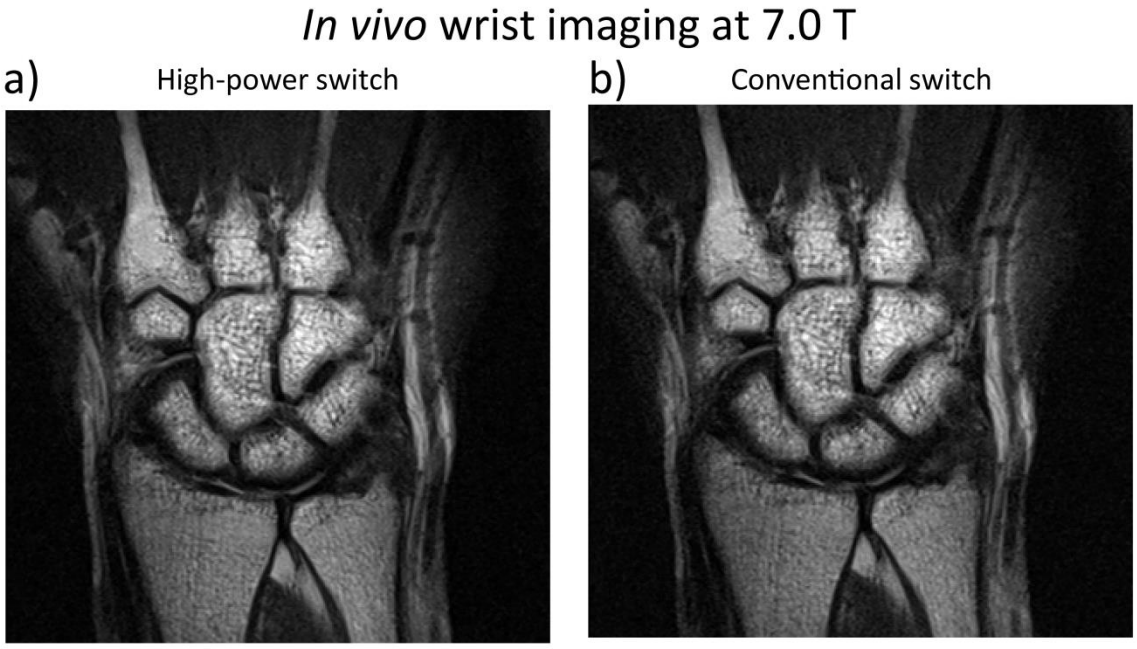

Figure 6 –*In vivo* wrist MRI at 7.0T using a rapid acquisition with relaxation enhancement (RARE) technique: in plane resolution=(0.3x0.3)mm^2, slice thickness=3mm, matrix size=(320x320)mm^2, number of slices=11, TR=3000ms, TE=59ms, nominal flip angle=150°, P_{peak}=223W, P_{avg}=10W, total scan time=149s. **a)** acquired with the high-power Tx/Rx switch and **b)** acquired with the conventional Tx/Rx switch.

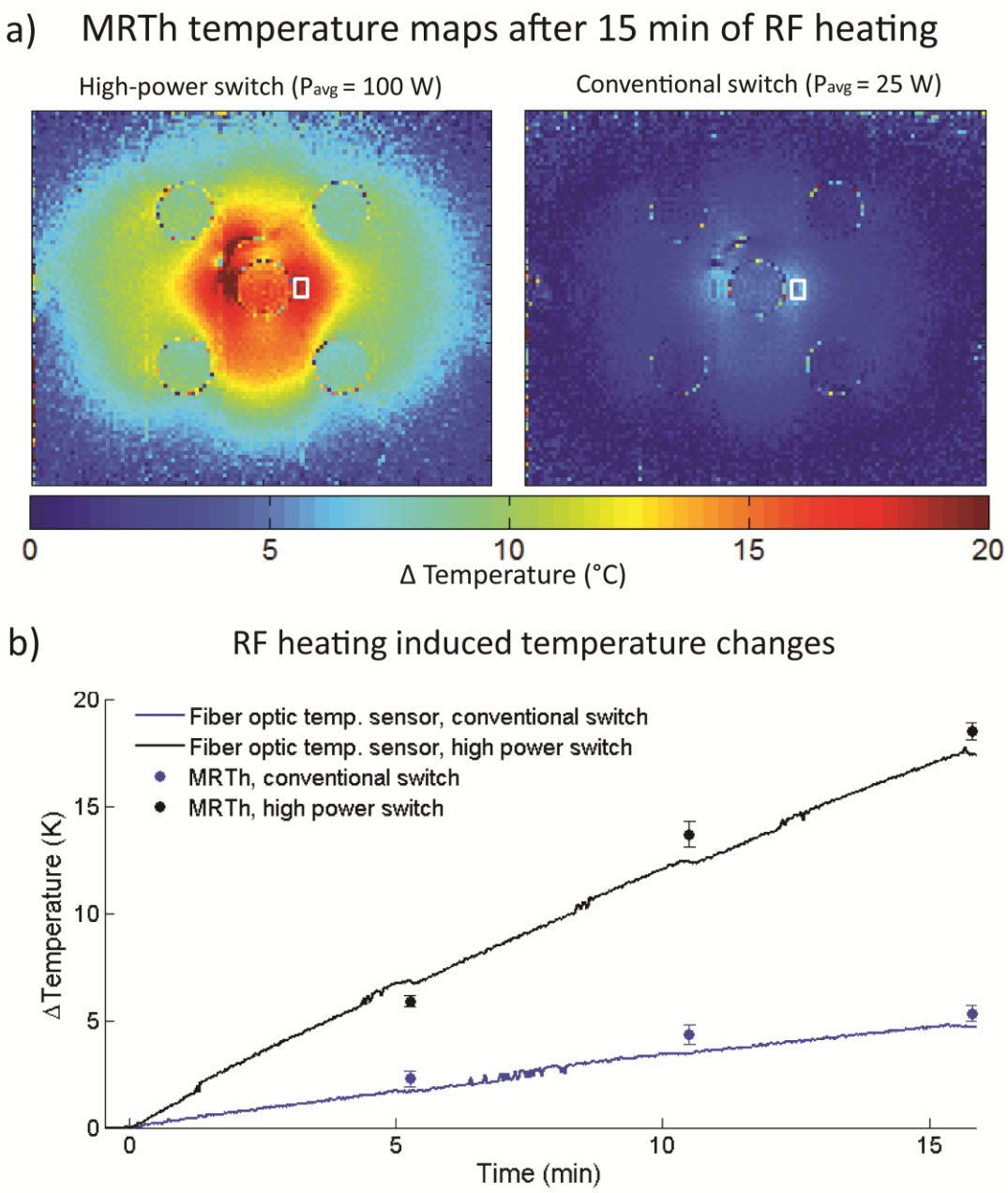

Figure 7 – a) Temperature maps obtained from MR thermometry (in plane resolution=(1.5x1.5)mm^2, slice thickness=4mm, matrix size=(192x192), number of slices=3, TR=61ms, TE1=2.26ms and TE2=11.44ms, nominal flip angle=30°, total scan time=11s) after 15min of RF heating with the high-power Tx/Rx switch and P_{avg}=100W at the antenna feeding point (left) and with the conventional Tx/Rx switch and P_{avg}=25W at the antenna feeding point (right). **b)** RF heating induced temperature changes at depth of 15mm in the phantom monitored with MR thermometry (evaluated in the white rectangle in b)) and fiber optic probes (FOP).

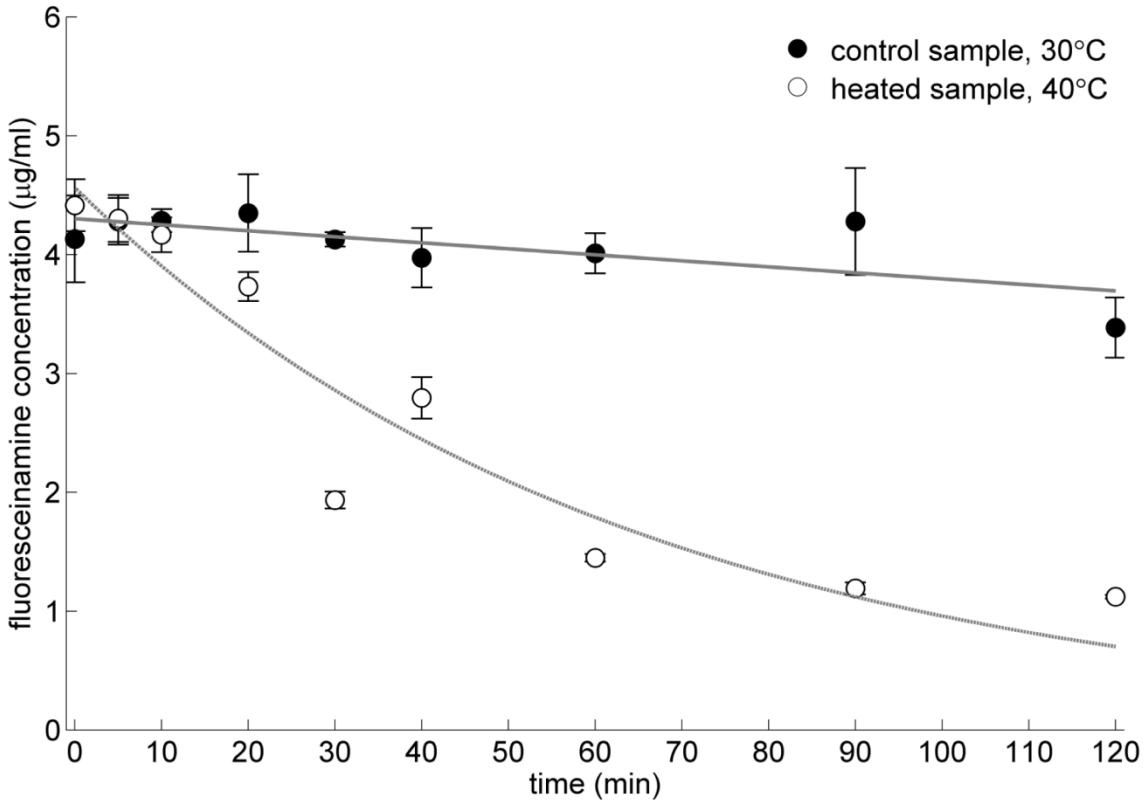

Figure 8 – Release of fluoresceinamine from the thermoresponsive polymers after RF heating. After reaching 40°C in the heated sample, the release of fluoresceinamine was monitored over 120min. The control sample, maintained at 30°C (>LCST=34°C), showed a very slow release. This is mainly due to slow hydrolysis of Schiff base bonds that attach fluoresceinamine to the polymer. The heated sample, subject to a higher temperature and above LCST of the polymer, showed higher release rate; 68% after 60min. In this case, the Schiff base bond was hydrolyzed faster at higher temperatures and the contraction of the polymer upon T>LCST increased the release of fluoresceinamine.

References

1. Wust P, Hildebrandt B, Sreenivasa G, Rau B, Gellermann J, Riess H, Felix R, Schlag PM. Hyperthermia in combined treatment of cancer. The lancet oncology 2002;3(8):487-497.
2. Horsman MR, Overgaard J. Hyperthermia: a potent enhancer of radiotherapy. Clin Oncol (R Coll Radiol) 2007;19(6):418-426.
3. Issels RD, Lindner LH, Verweij J, Wust P, Reichardt P, Schem BC, Abdel-Rahman S, Daugaard S, Salat C, Wendtner CM. Neo-adjuvant chemotherapy alone or with regional hyperthermia for localised high-risk soft-tissue sarcoma: A randomised phase 3 multicentre study. Lancet Oncol 2010;11(6):561-570.
4. Lee Titsworth W, Murad GJ, Hoh BL, Rahman M. Fighting fire with fire: the revival of thermotherapy for gliomas. Anticancer Res 2014;34(2):565-574.
5. Issels RD, Lindner LH, Verweij J, Wust P, Reichardt P, Schem B-C, Abdel-Rahman S, Daugaard S, Salat C, Wendtner C-M. Neo-adjuvant chemotherapy alone or with regional hyperthermia for localised high-risk soft-tissue sarcoma: a randomised phase 3 multicentre study. The Lancet Oncology 2010;11(6):561-570.
6. McDaniel JR, Dewhirst MW, Chilkoti A. Actively targeting solid tumours with thermoresponsive drug delivery systems that respond to mild hyperthermia. International journal of hyperthermia : the official journal of European Society for Hyperthermic Oncology, North American Hyperthermia Group 2013;29(6):501-510.
7. Chilkoti A, Dreher MR, Meyer DE, Raucher D. Targeted drug delivery by thermally responsive polymers. Advanced drug delivery reviews 2002;54(5):613-630.
8. Langereis S, Keupp J, van Velthoven JL, de Roos IH, Burdinski D, Pikkemaat JA, Grüll H. A temperature-sensitive liposomal 1H CEST and 19F contrast agent for MR image-guided drug delivery. Journal of the American Chemical Society 2009;131(4):1380-1381.
9. Peller M, Schwerdt A, Hossann M, Reinl HM, Wang T, Sourbron S, Ogris M, Lindner LH. MR characterization of mild hyperthermia-induced gadodiamide release from thermosensitive liposomes in solid tumors. Investigative radiology 2008;43(12):877-892.
10. Mao Z, Ma L, Yan J, Yan M, Gao C, Shen J. The gene transfection efficiency of thermoresponsive N, N, N-trimethyl chitosan chloride-g-poly (N-isopropylacrylamide) copolymer. Biomaterials 2007;28(30):4488-4500.
11. Twaites BR, de las Heras Alarcón C, Cunliffe D, Lavigne M, Pennadam S, Smith JR, Górecki DC, Alexander C. Thermo and pH responsive polymers as gene delivery vectors: effect of polymer architecture on DNA complexation in vitro. Journal of controlled release 2004;97(3):551-566.
12. Lu Y, Sun W, Gu Z. Stimuli-responsive nanomaterials for therapeutic protein delivery. Journal of controlled release 2014;194:1-19.
13. Ishihara Y, Calderon A, Watanabe H, Okamoto K, Suzuki Y, Kuroda K, Suzuki Y. A precise and fast temperature mapping using water proton chemical shift. Magnetic Resonance in Medicine 1995;34(6):814-823.
14. Rieke V, Butts Pauly K. MR thermometry. Journal of Magnetic Resonance Imaging 2008;27(2):376-390.
15. Wonneberger U, Schnackenburg B, Wlodarczyk W, Walter T, Streitparth F, Rump J, Teichgräber UK. Intradiscal temperature monitoring using double gradient-echo pulse sequences at 1.0 T. Journal of Magnetic Resonance Imaging 2010;31(6):1499-1503.
16. McDannold N, Tempany CM, Fennessy FM, So MJ, Rybicki FJ, Stewart EA, Jolesz FA, Hynynen K. Uterine leiomyomas: MR imaging–based thermometry and thermal dosimetry during focused ultrasound thermal ablation. Radiology 2006;240(1):263-272.

17. Winter L, Özerdem C, Hoffmann W, Santoro D, Müller A, Waiczies H, Seemann R, Graessl A, Wust P, Niendorf T. Design and Evaluation of a Hybrid Radiofrequency Applicator for Magnetic Resonance Imaging and RF Induced Hyperthermia: Electromagnetic Field Simulations up to 14.0 Tesla and Proof-of-Concept at 7.0 Tesla. PLOS ONE 2013;8(4):e61661.
18. Winter L, Oezerdem C, Hoffmann W, van de Lindt T, Periquito J, Ji Y, Ghadjar P, Budach V, Wust P, Niendorf T. Thermal magnetic resonance: physics considerations and electromagnetic field simulations up to 23.5 Tesla (1GHz). Radiation Oncology 2015;10(1):201.
19. Winter L, Niendorf T. Electrodynamics and radiofrequency antenna concepts for human magnetic resonance at 23.5 T (1 GHz) and beyond. Magnetic Resonance Materials in Physics, Biology and Medicine 2016;29(3):641-656.
20. Niendorf T, Oezerdem C, Ji Y, Oberacker E, Kuehne A, Waiczies H, Winter L. Radiative RF Antenna Arrays for Cardiac, Brain and Thermal Magnetic Resonance at Ultrahigh and Extreme Magnetic Field Strengths: Concepts, Electromagnetic Field Simulations and Applications. Verona, Italy: Proceedings ICEAA - IEEE APWC 2017; 2017; Abstract 670
21. Doherty W, Joos R. The pin diode circuit designers' handbook. Microsemi Corporation 1998;1.
22. Xiao Y, Zhao Z, Qian Z, Zhou H. A high isolation switching unit for MRI system. Procedia Engineering 2010;7:265-269.
23. Brunner DO, Furrer L, Weiger M, Baumberger W, Schmid T, Reber J, Dietrich BE, Wilm BJ, Froidevaux R, Pruessmann KP. Symmetrically biased T/R switches for NMR and MRI with microsecond dead time. Journal of Magnetic Resonance 2016;263:147-155.
24. Thapa B, Kaggie J, Sapkota N, Frank D, Jeong EK. Design and Development of a General-Purpose Transmit/Receive (T/R) Switch for 3T MRI, Compatible for a Linear, Quadrature and Double-Tuned RF Coil. Concepts in Magnetic Resonance Part B: Magnetic Resonance Engineering 2016;46(2):56-65.
25. Watkins R, Caverly R, Doherty W. 298MHz Micro miniature 2KW Transmit Receive Switch for 7.0 Tesla TR Arrays. 2012; Abstract 2686
26. Ji Y, Hoffmann W, Pham M, Oezerdem C, Waiczies H, Niendorf T, Winter L. Higher is better: High peak and high average RF power transmit/receive switch for an integrated RF heating applicator operating at 297 MHz (7.0 Tesla). 2017. Proceedings of the 25th Annual Meeting of ISMRM, #5432.
27. White JF, Mortenson KE. Diode SPDT switching at high power with octave microwave bandwidth. IEEE Transactions on Microwave Theory and Techniques 1968;16(1):30-36.
28. Carr J. The technician's radio receiver handbook: wireless and telecommunication technology: Newnes; 2001.
29. Oezerdem C, Winter L, Graessl A, Paul K, Els A, Weinberger O, Rieger J, Kuehne A, Dieringer M, Hezel F. 16-channel bow tie antenna transceiver array for cardiac MR at 7.0 tesla. Magnetic Resonance in Medicine 2015.
30. Dunn AE, Dunn DJ, Macmillan A, Whan R, Stait-Gardner T, Price WS, Lim M, Boyer C. Spatial and temporal control of drug release through pH and alternating magnetic field induced breakage of Schiff base bonds. Polymer Chemistry 2014;5(10):3311-3315.
31. Fujii T, Akasegawa A, Amatatsu S, Moriwaki M, Shigematsu H, Irie H, Hayashi H, Shimizu T, Satou R. Over 200-W high isolation GaN-switch for L-band radar module. 2011. IEEE. p 25-28.
32. Choi SD. High-power microstrip RF switch. JAPL Quart Tech Rev 1971;1(3):110-124.
33. Winter L, Oberacker E, Paul K, Ji Y, Oezerdem C, Ghadjar P, Thieme A, Budach V, Wust P, Niendorf T. Magnetic resonance thermometry: methodology, pitfalls and practical solutions. International Journal of Hyperthermia 2016;32(1):63-75.